Environmental Science & Technology

Article

pubs.acs.org/est

Speciation of Radioactive Soil Particles in the Fukushima Contaminated Area by IP Autoradiography and Microanalyses

Hiroki Mukai,*[,†] Tamao Hatta,[‡] Hideaki Kitazawa,[§] Hirohisa Yamada,[∥] Tsuyoshi Yaita,[⊥] and Toshihiro Kogure[†]

[†]Department of Earth and Planetary Science, Graduate School of Science, The University of Tokyo, 7-3-1 Hongo, Bunkyo-ku, Tokyo, 113-0033, Japan

[‡]Japan International Research Center for Agricultural Sciences, 1-1 Ohwashi, Tsukuba, Ibaraki 305-8686, Japan

[§]Quantum Beam Unit, National Institute for Materials Science, 1-2-1 Sengen, Tsukuba, Ibaraki 305-0047, Japan

[∥]Environmental Remediation Materials Unit, National Institute for Materials Science, 1-1 Namiki, Tsukuba, Ibaraki 305-0044, Japan

[⊥]Quantum Beam Science Center and Fukushima Environmental Safety Center, Japan Atomic Enegy Agency, 1-1-1 Kouto, Sayo-cho, Sayo-gun, Hyogo 679-5148, Japan

Supporting Information

ABSTRACT: Radioactive soil particles several tens of micrometers in size were collected from litter soil in the radiation contaminated area by the Fukushima nuclear plant accident and characterized using electron and X-ray microanalyses. The radioactive particles were discriminated by autoradiography using imaging plates (IP) on which microgrids were formed by laser ablation in order to find the particles under microscopy. Fifty radioactive particles were identified and classified into three types from their morphology and chemical composition, namely: (1) aggregates of clay minerals, (2) organic matter containing clay mineral particulates, and (3) weathered biotite originating from local granite. With respect to the second type, dissolution of the organic matter did not reduce the radiation, suggesting that the radionuclides were also fixed by the clay minerals. The weathered biotite grains have a plate-like shape with well-developed cleavages inside the grains, and kaolin group minerals and goethite filling the cleavage spaces. The reduction of the radiation intensity was measured before and after the trimming of the plate edges using a focused ion beam (FIB), to examine whether radioactive cesium primarily sorbed at frayed edges. The radiation was attenuated in proportion to the volume decrease by the edge trimming, implying that radioactive cesium was sorbed uniformly in the porous weathered biotite.

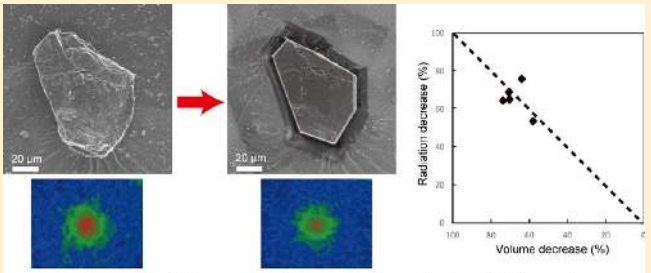

The results of edge-removal treatment for radioactive biotite grains

INTRODUCTION

The accident at the Fukushima-Daiichi nuclear power plant in March 2011 released a significant amount of radionuclides, including cesium (Cs), which contaminated forests, fields, residences, rivers, and ponds. Three years after the accident, radioactive cesium is the major source of the radiation at Fukushima area. Hence, it is necessary to trace its precise behavior in the environment.

Radioactive cesium contamination has also occurred at the Hanford site in southeastern Washington, U.S.A. and over a vast area of Europe and western Russia, following the Chernobyl accident in May of 1986. These accidents triggered and accelerated studies on the environmental behavior of radioactive cesium. Many researchers have suggested, mainly based on laboratory experiments, that micaceous minerals are important for sorption and retention of Cs in the ground or soil.[1−6] For instance, Cornel et al.[4] summarized the potential sorption sites for Cs^+ in the micaceous minerals as follows; (1) cation exchange sites on the surface, (2) layer edge sites, (3) frayed edge sites (FES), and (4) original interlayer sites inside the crystal. A number of studies have suggested that FES, which formed around the edges of plate-like mica crystals during weathering, strongly and selectively sorb Cs.[7−9] Recently, however, Kogure et al.[10] and Okumura et al.[11] used high-resolution transmission electron microscopy (HRTEM) to directly observe Cs ions sorbed deeply in the interlayer region of vermiculite and phlogopite.

Although these experimental results are valuable, it is uncertain whether they are applicable to Fukushima and other areas, as the concentration of radioactive cesium in the contaminated sites is far lower ($\sim 10^{-10}$) than the concentrations used in the laboratory experiments. Consequently, given such low Cs concentrations and the potential presence of competing phases or elements, micaceous minerals may not be the major absorbent of radioactive cesium at Fukushima. Further, Cs may sorb

Received: June 12, 2014
Revised: October 21, 2014
Accepted: October 24, 2014

   dx.doi.org/10.1021/es502849e | Environ. Sci. Technol. XXXX, XXX, XXX−XXX

preferentially to different mica sorption sites at low versus high concentrations of Cs. Nonetheless, in order to better understand the fate and transport of radioactive cesium at Fukushima and develop effective methods of decontamination, it is fundamentally important to know the materials/phases which retain radioactive cesium.

The low concentration of radioactive cesium in the soil at Fukushima precludes specifying its location, even using advanced microanalytical techniques such as X-ray microanalysis with synchrotron radiation. In the present study, we used imaging plate (IP) autoradiography to locate the radioactive particles. Utilization of IP instead of silver halide films for radiation recording is especially useful since the IP has higher sensitivity and yields better quantification of radiation.[12,13] The radioactive particles dispersed on the IP were then selected for characterization with scanning and transmission electron microscopy (SEM/TEM). Moreover, we applied different treatments to the particles to explore the intraparticle distribution of radioactive cesium.

SAMPLES AND METHODS

A litter soil sample was collected from fallen leaves on the ground of a forest near the boundary between Iitate village and Namie town in Fukushima, Japan. The sample was dried in an oven and sieved to 20−75 μm size particles using a sieve shaker. The radiation intensity of these particles was 1400 ± 1 Bq/g for Cs-137 and 727 ± 1 Bq/g for Cs-134, as measured with a germanium γ-ray spectrometer (GEM15P4−70, Seiko EG&G). These values correspond to the radioactive Cs concentration of 0.45 ppb in the sample. In the spectrum from the particles, peaks of the γ-rays from Cs-137 and Cs-134 were extremely higher than those from other radionuclides (Supporting Information (SI) Figure S1). X-ray diffraction (XRD, Rigaku Ultima$^+$ with CuKα radiation) identified quartz, plagioclase, and hornblende, as well as the broad peak around 2θ = 20° from phyllosilicates with low crystallinity, namely clay minerals (Figure 1). In the low 2θ region, broad 14.1, 10.0, and 7.2 Å peaks were identified. The particles were suspended in ethanol and dispersed on 100 × 80 mm^2 imaging plates (IPs) (FDL-UR-V, Fuji Film) with microgrid pattern. The patterning was formed by laser ablation using a YVO_4 laser maker (532 nm) (Figure 2), performed by L-TEC Inc., Tokyo. The microgrid consists of ablation holes of ~80 μm in diameter and 200 or 250 μm pitch, and ablation lines of 5 mm pitch. The phosphor coating was stimulated, probably during laser ablation. This microgrid pattern also appeared in the read-out image of the IP, superimposed with spots formed by the radiation from radioactive particles. Accordingly, the radioactive particles were located easily with an optical microscope. The IPs were kept in the dark for about a month of exposure to radiation and then read with an IP reader (FLA-7000, Fuji Film). The radioactive particles were located using a high-magnification stereomicroscope and then picked up and transferred onto different substrates by a micromanipulator (Quick Pro, Micro Support Co., Ltd.) and vacuum tweezers (VP-SET-2, Micro Support Co., Ltd.). For confirmation, the radiation intensities of the transferred radioactive particles were measured by covering the particles on the substrates with an IP (SI Figure S2).

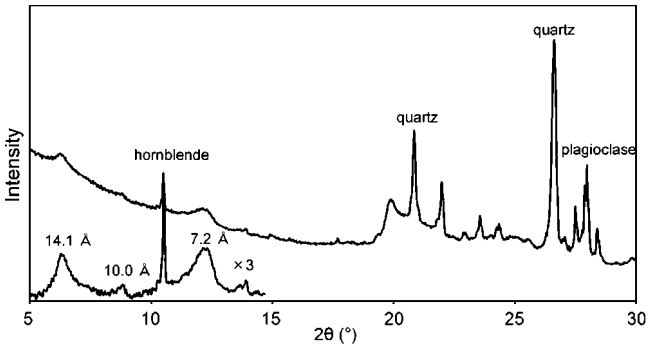

Figure 1. XRD pattern of the litter soil particles of 20−75 μm in size, collected from the ground of forest in the Fukushima contaminated area. The vertically magnified and background-subtracted pattern is shown at the bottom-left.

The radioactive particles were then analyzed by SEM (Hitachi S-4500) equipped with an energy-dispersive X-ray spectrometer (EDS) with an ultrathin window (Kevex Sigma). The particles were carbon-coated before the analyses. The SEM observations and the EDS measurements were performed with an acceleration voltage of 15 kV. During the acquisition of the spectra for about 2 min, the electron beam was scanned within a square covering more than a half of the area over a particle. Further, TEM characterization was performed using a JEOL JEM-2010UHR TEM operated at 200 kV and equipped with an energy-dispersive X-ray spectrometer (EDS) with an ultrathin window. The TEM specimens were prepared using a focused ion beam (FIB) system (Hitachi FB-2100).

RESULTS

Selection of Radioactive Particles. Figure 3a shows an IP read-out image one month after the soil particles were dispersed on the IP. Many bright spots over which radioactive particles are expected to exist can be observed. Observation of the corresponding areas by the stereomicroscope easily located the radioactive particles (Figure 3b−d). These grains were transferred onto other substrates such as glass slides or conductive double-stick tape. As shown in Figure 3b−d, the radii of spots in the IP images are generally several times larger than the associated particles because the radiation is emitted in all directions and the phosphor layer is 150-μm thick. Dispersed particles were occasionally so close that distinguishing the radioactive particles was ambiguous. To solve this problem, the particles of interest transferred to the substrate were covered with an IP for about a week, and then the IP was read-out to confirm that they were radioactive (SI Figure S2).

Microanalyses. Using the method described above, 50 radioactive particles were collected and were initially analyzed using SEM-EDS. From their appearance and chemical composition, they can be roughly classified into three types.

The first type, which accounts for 14 particles, is an aggregation of mineral particulates (Figure 4). EDS spectra indicated the abundance of oxygen, silicon, and aluminum, implying aluminum silicates as constituting minerals. Several specimens were thinned using FIB and characterized with TEM. An example is shown in Figure 5. The aggregate is porous, and quartz, biotite, chlorite, and kaolin group minerals (KGMs) were suggested from the EDS analyses.

Twenty particles are of the second type, which is characterized by intense carbon and oxygen peaks in the EDS spectra, indicating that organic matter is the main constituent (Figure 6). However, relatively minor aluminum and silicon peaks indicate a mixture of organic matter and clay minerals. TEM-FIB analysis revealed clay fragments or particulates of biotite, KGM, and quartz embedded in organic matter (Figure 7a). To determine the host of radioactive cesium, the organic component was

dx.doi.org/10.1021/es502849e | Environ. Sci. Technol. XXXX, XXX, XXX−XXX

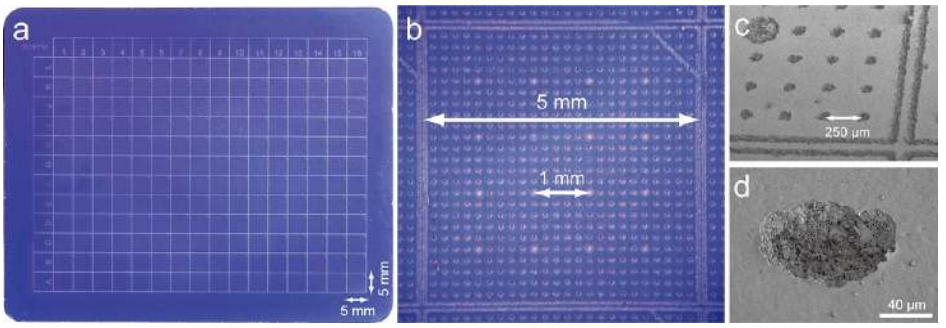

Figure 2. (a) Imaging plate (IP) with a microgrid pattern, used for the identification of radioactive particles. (b) Magnified image of the IP, showing the grid pattern of a 5 mm square. (c, d) Oblique-perspective SEM images of the IP with the grids.

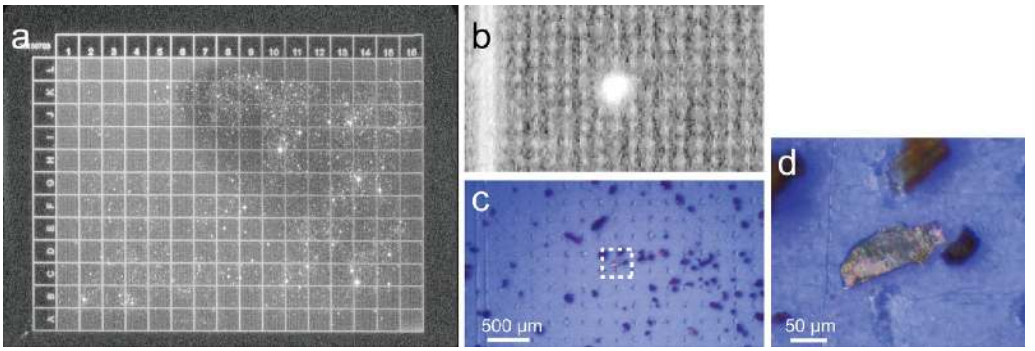

Figure 3. (a) IP read-out image after one month of exposure to radiation from dispersed soil particles. (b) Magnified image of (a) showing bright spots formed by radiation. (c) Stereomicroscope image corresponding to the area of (b). (d) Magnified stereomicroscope image from the rectangular in (c) showing a radioactive soil particle.

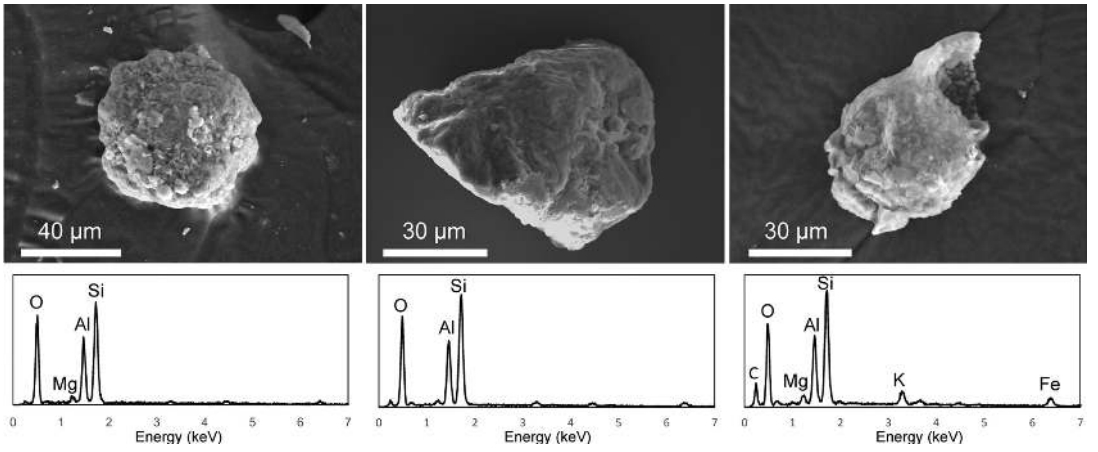

Figure 4. SEM images (upper) and EDS spectra (lower) of the first type of particle, namely aggregates of clay minerals.

dissolved by dropping sodium hypochlorite onto the particles placed on glass fiber filter, and the change of radiation was measured with IP (Figure 7b,c). The EDS spectra confirmed dissolution of the organic matter, but the intensity of radiation was similar, suggesting that radioactive cesium was fixed to the clay minerals rather than the organic matter (Figure 7).

The third type, represented by 16 particles, has the plate-like morphology expected of single-crystal phyllosilicates (Figure 8). The EDS spectra contain O, Mg, Al, Si, K, Ti, and Fe peaks, consistent with biotite, but often the relative intensity of Al is higher than that expected for biotite, likely reflecting the formation of KGMs within the cleavage spaces, as described below. Although they appear to be single-crystal, TEM images, and EDS from cross sections of the plates (Figure 9a,b) indicated that KGMs and goethite was formed inside the cleavage spaces of biotite, yielding a laminate structure. These mineral phases were confirmed by electron diffraction patterns (SI Figure S3). As mentioned above, it has been reported that micaceous minerals efficiently retain cesium, especially at frayed edges.[8] To examine whether this result is relevant for radioactive cesium retained in the micas at Fukushima, we conducted an experiment with FIB: After measuring the radiation of the biotite plates using IP, the edges of the plates were trimmed back by Ga sputtering, and then the radiation was measured again (Figure 9c,d). Although the radiation intensity was reduced after the removal of the edges, the decrease in activity was proportional to the volume removed (Figure 9e). This suggests that radioactive cesium is not

dx.doi.org/10.1021/es502849e | Environ. Sci. Technol. XXXX, XXX, XXX−XXX

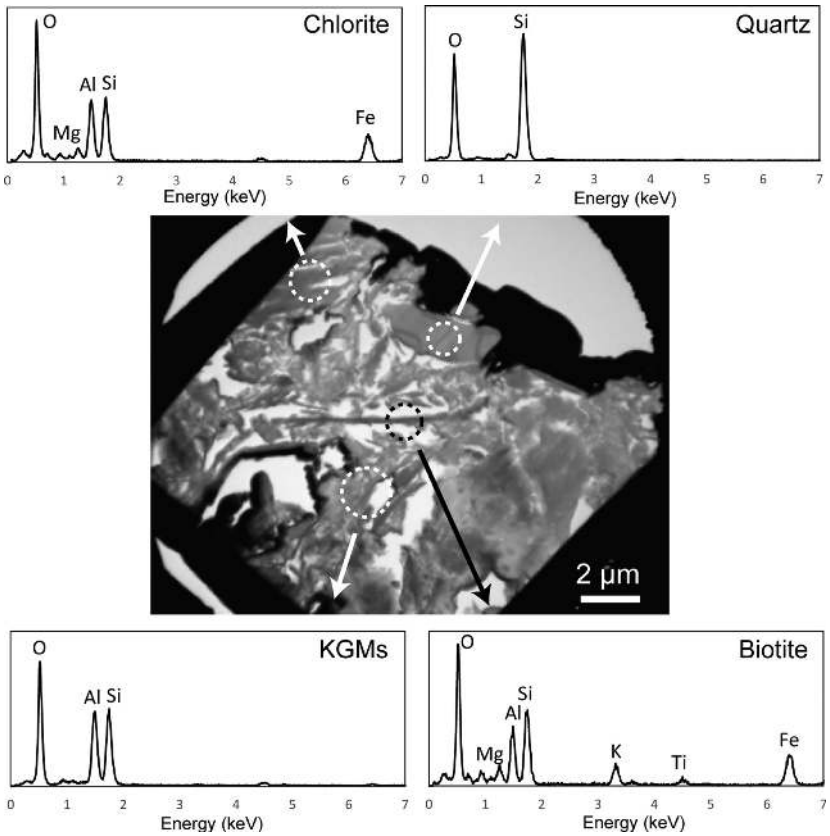

Figure 5. TEM-EDS analyses of the particle classified as the first type. Quartz, biotite, chlorite, and kaolin group minerals (KGMs) are suggested from EDS analyses.

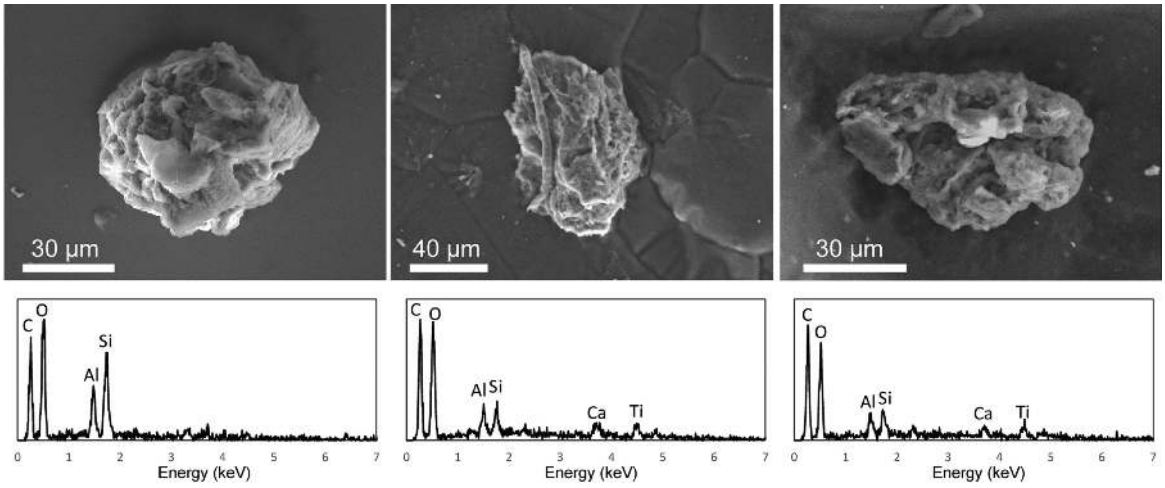

Figure 6. SEM images (upper) and EDS spectra (lower) of the second type of particle in which organic matter is abundant.

concentrated only at the edges, but also extends into the plate-like crystals, probably through the cleavage spaces.

Finally, we confirmed using the γ-ray spectrometer that the radioactive particles located by the IP autoradiography really contain Cs-134 and -137, because natural radionuclides like K-40, uranium, or the thorium series can also excite imaging plates. A few of the radioactive biotite particles were set in the spectrometer, and the radiation was measured for 200 000 s with and without the particles. As shown in the figure, although several kinds of γ rays were recorded, as well as those from radioactive cesium, they almost disappeared by the subtraction of the spectrum for "blank" (Figure 10), indicating that only the γ rays from radioactive cesium were emitted from the particles, and the others came from the environment. The same measurement was performed for the other two types of radioactive particles (aggregate of clay minerals and organic-dominant substance), and the existence of radioactive cesium was confirmed also in these particles (SI Figure S4).

DISCUSSION

Autoradiography using dedicated IPs with microgrids successfully discriminated radioactive soil particles, and SEM/TEM microanalyses elucidated their identities. Although IP itself cannot distinguish radionuclide species, it is probable that the

dx.doi.org/10.1021/es502849e | Environ. Sci. Technol. XXXX, XXX, XXX−XXX

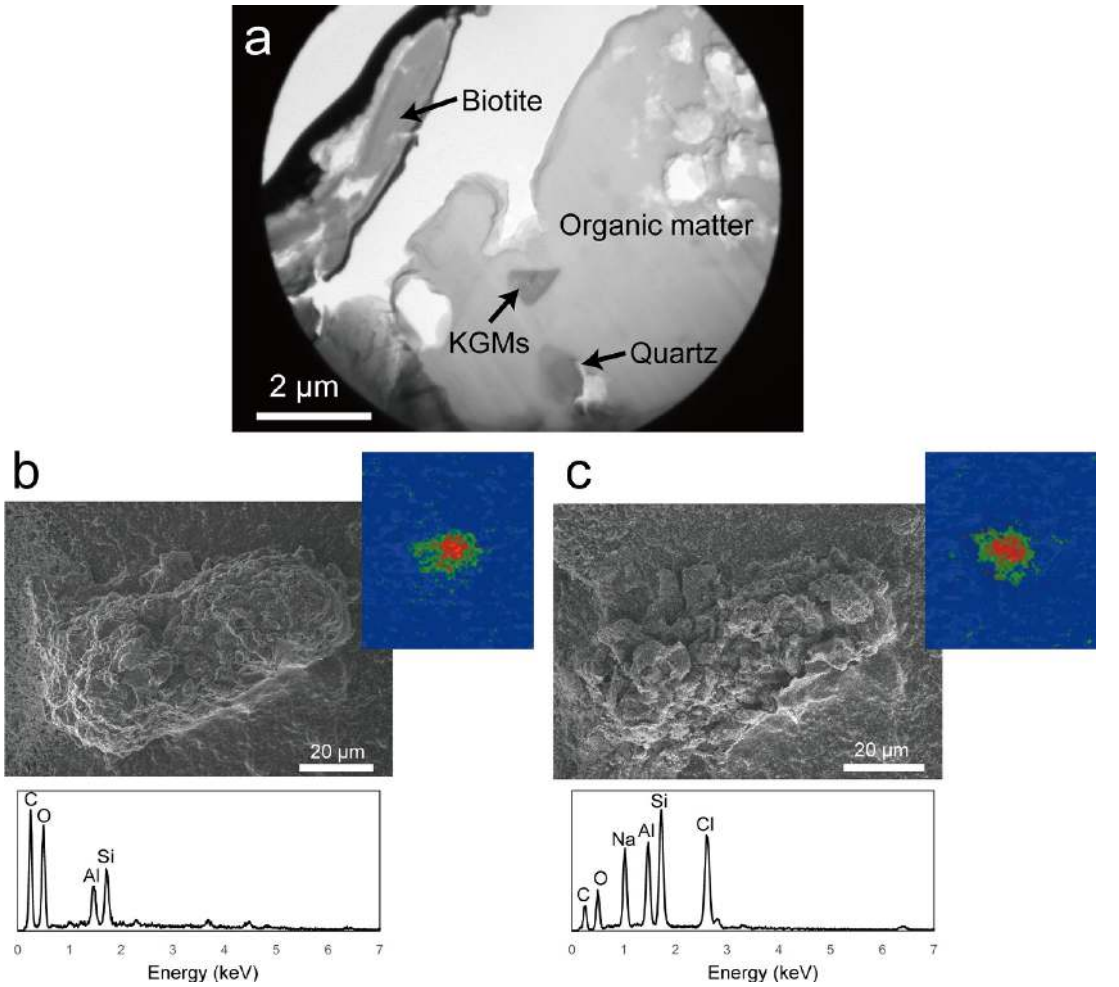

Figure 7. (a) TEM image of the second type of particle, showing organic matter and particulates of biotite, KGM, and quartz. (b, c) The result of bleaching treatment, showing SEM images (upper), read-out IP images from the particle (upper right), and EDS spectra obtained from the particle (lower), (b) before, and (c) after the treatment. Na and Cl detected in the EDS in (c) are probably from sodium hypochlorite.

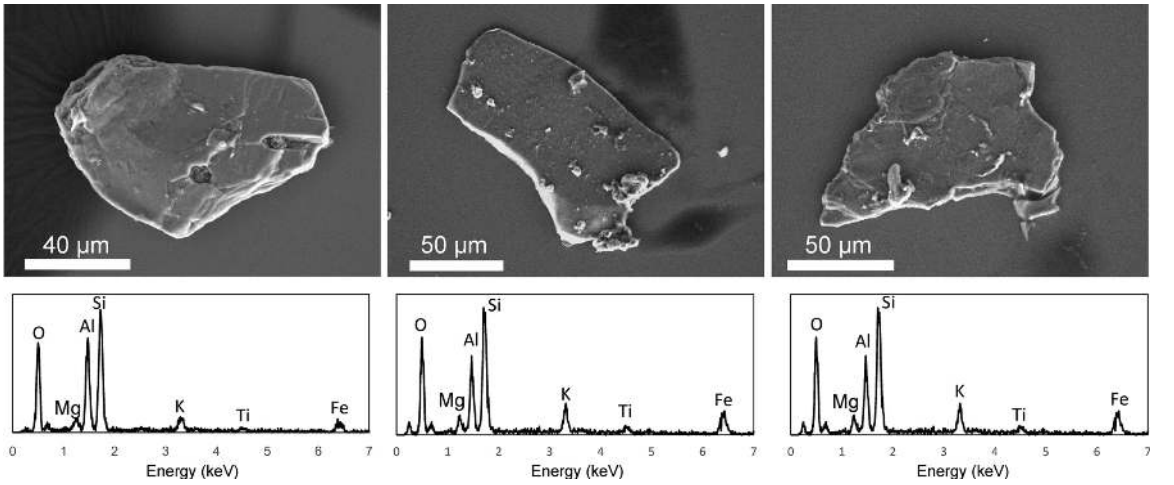

Figure 8. SEM images (upper) and EDS spectra (lower) of the third type of particle (weathered biotite).

origin of the radioactivity of these particles is Cs-137 and -134, because of their overwhelming abundance compared to other radionuclides (SI Figure S1). Accordingly, the following discussion is advanced on the assumption that radioactive Cs is sorbed in the particles.

The 50 radioactive particles were divided into three types. The first type, microaggregates of fine particulates of clay and other minerals, are probably water-stable and are described aggregates in the soil science literature.[14−16] These aggregates are generally 20−250 μm in diameter and consist largely of smaller particles like clay minerals, bonded together by various cements including

dx.doi.org/10.1021/es502849e | *Environ. Sci. Technol.* XXXX, XXX, XXX−XXX

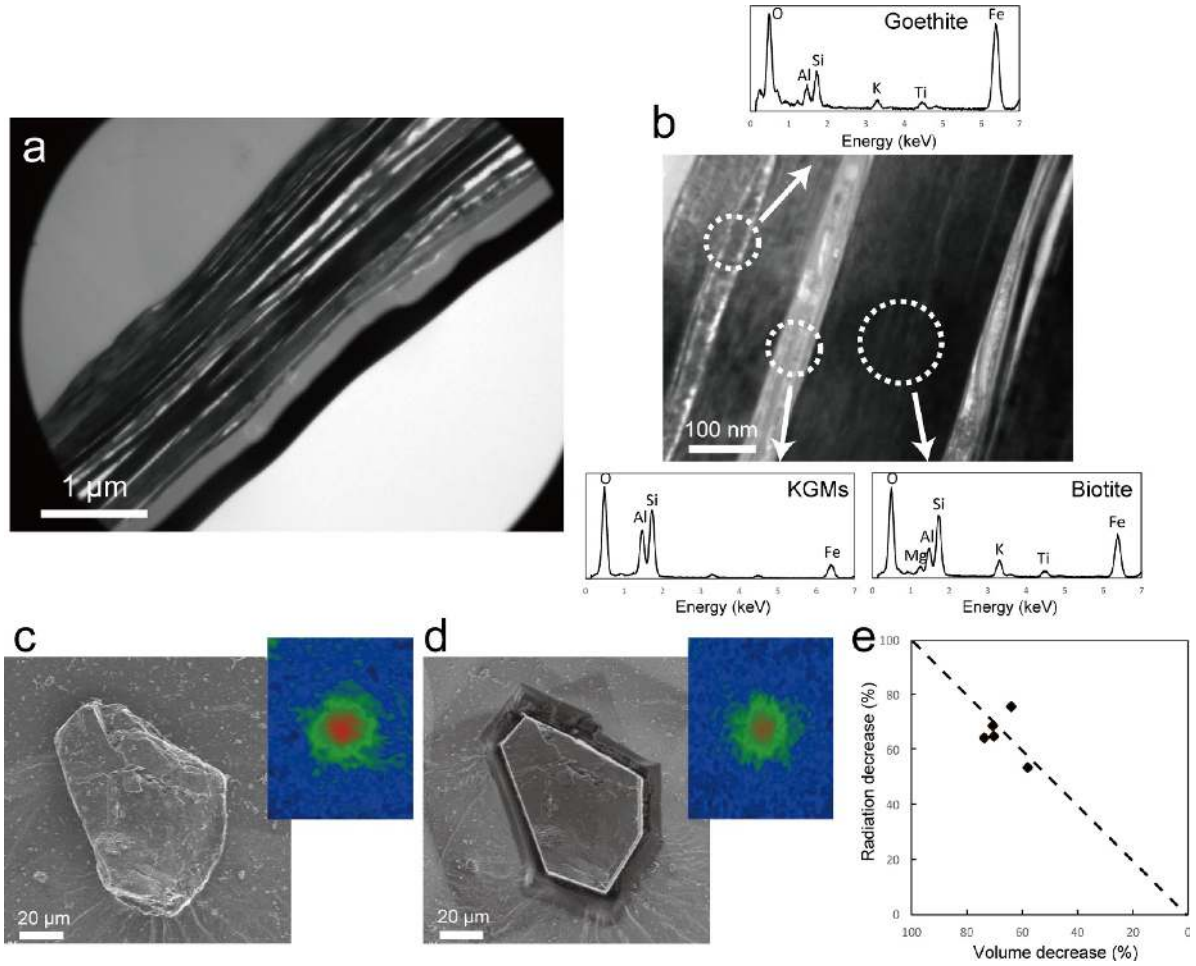

Figure 9. (a) Cross-sectional TEM image of the weathered biotite. (b) Magnified TEM image and EDS from each portion of the particle. KGMs and goethite are formed inside the cleavage spaces of the biotite. (c, d) An example of the edge-removal treatment. SEM images of the particle and read-out IP images (upper right), (c) before and (d) after the edge-removal. (e) The results of the edge-removal treatment for five radioactive biotite grains. The volume and radiation reductions by the edge-removal are almost proportional, indicating that radionuclides are not concentrated around the edges but distributed rather homogeneously in the grain.

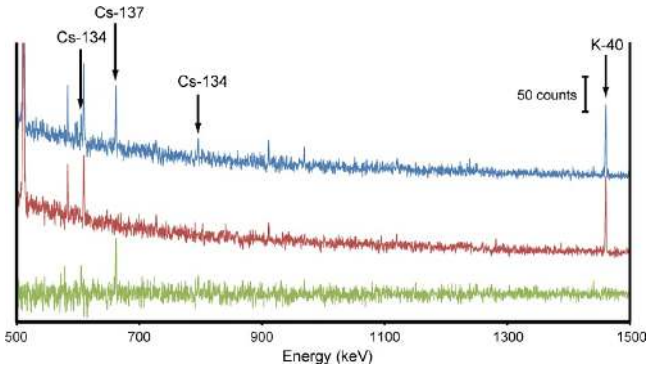

Figure 10. γ-ray spectra from radioactive biotite particles (top), "blank" (center), and subtraction of the latter from the former (bottom). The duration time for the measurement was 200 000 s. Note that only peaks for Cs-134 and -137 are detectable in the subtracted spectrum.

organic matter related to plant, fungi, bacteria, etc., crystalline oxides, or highly disordered aluminum silicates.[15] TEM examination showed that such aggregates are very porous and have a large specific surface area (Figure 5). If these soil aggregates contact a solution containing radioactive cesium, then the solution will be infiltrated inside the aggregates with capillary action, and the cesium will be sorbed to appropriate sites of the constituting clay minerals.

The second type of radioactive soil particles may be related to the egestion of soil organisms. Organisms such as small arthropods, eating mainly fallen leaves, may produce organic-dominant excrement containing clay minerals ingested accidentally.

The altered biotite crystals that constitute the third type of radioactive particles are weathered products of Abukuma and Kitakami granite−granodiorite bodies that formed in the early Cretaceous and are ubiquitous in the eastern part of Fukushima Prefecture.[17,18] Quartz, plagioclase, and hornblende identified in the XRD pattern (Figure 1) are of the same origin. KGMs and goethite in the cleaved spaces of biotite are secondary minerals formed from weathering of biotite and (probably) plagioclase in granite. The biotite crystals are probably biotite−vermiculite (B−V) mixed-layer minerals formed by weathering; the 14.1 and 10.0 Å peaks in Figure 1 correspond to vermiculite-like and biotite layers, respectively. Weathered micas (vermiculite or B−V mixed layer minerals) have been reported to be effective Cs sorbents.[19,20] However, there is a possibility that KGMs also fix the cesium ions because KGMs have a certain level of capacity to sorb cesium ions, as indicated in a database recently reported after the Fukushima accident.[21] As mentioned above, previous

dx.doi.org/10.1021/es502849e | Environ. Sci. Technol. XXXX, XXX, XXX−XXX

studies have suggested that Cs ions are fixed preferentially at frayed edges of weathered mica. However, our experimental results using FIB indicate that this observation does not apply at Fukushima. One reason may be that these weathered biotites are so porous (Figure 9a) that the solutions bearing radioactive Cs infiltrated rapidly into the cleaved zones spaces by capillary action.

■ ASSOCIATED CONTENT

Supporting Information

Figure S1. γ-ray spectrums from the litter soil particles, collected from the ground of forest in the Fukushima contaminated area. Figure S2. (a) Eleven soil particles with possibility to be radioactive, picked up and transferred onto conductive double-stick tape. (b) Read-out image of an IP which covered the tape in (a) for a week. Figure S3. Examples of electron diffraction patterns obtained from the third type, e.g. radioactive plate-like particles, to confirm the mineral phases. Figure S4. SEM images (top), EDS spectra (center) and γ-ray spectra (bottom) from (a) the first type (aggregates of clay minerals) and (b) the second type (organic matter dominant) radioactive particles described in the text. This material is available free of charge via the Internet at http://pubs.acs.org.

■ AUTHOR INFORMATION

Corresponding Author

*Phone: +81-3-5841-4019; fax: +81-3-5841-4019; e-mail:hmukai@eps.s.u-tokyo.ac.jp.

Notes

The authors declare no competing financial interest.

■ ACKNOWLEDGMENTS

The authors are grateful to several anonymous reviewers for their valuable comments, and M. Mitome in National Institute for Materials Science for several useful suggestions. A part of this work was supported by a Grant-in-Aid for scientific research (No. 24340133) from the Ministry of Education, Culture, Sports, Science, and Technology of Japan.

■ REFERENCES

(1) Francis, C. W.; Brinkley, F. S. Preferential adsorption of Cs-137 to micaceous minerals in contaminated freshwater sediment. *Nature* **1976**, *260*, 511−513.

(2) Evans, D. W.; Alberts, J. J.; Clark, R. A. Reversible ion-exchange fixation of cesium-137 leading to mobilization from reservoir sediments. *Geochim. Cosmochim. Acta* **1983**, *47*, 1041−1049.

(3) Comans, R. N. J.; Haller, M.; Depreter, P. Sorption of cesium on Illite—Non-equilibrium behavior and reversibility. *Geochim. Cosmochim. Acta* **1991**, *55*, 433−440.

(4) Cornell, R. M. Adsorption of cesium on minerals—A review. *J. Radioanal. Nucl. Chem.* **1993**, *171*, 483−500.

(5) Poinssot, C.; Baeyens, B.; Bradbury, M. H. Experimental and modelling studies of caesium sorption on Illite. *Geochim. Cosmochim. Acta* **1999**, *63*, 3217−3227.

(6) Zachara, J. M.; Smith, S. C.; Liu, C. X.; McKinley, J. P.; Serne, R. J.; Gassman, P. L. Sorption of Cs^+ to micaceous subsurface sediments from the Hanford site, U.S.A. *Geochim. Cosmochim. Acta* **2002**, *66*, 193−211.

(7) Brouwer, E.; Baeyens, B.; Maes, A.; Cremers, A. Cesium and rubidium ion equilibria in Illite Clay. *J. Phys. Chem.* **1983**, *87*, 1213−1219.

(8) McKinley, J. P.; Zachara, J. M.; Heald, S. M.; Dohnalkova, A.; Newville, M. G.; Sutton, S. R. Microscale distribution of cesium sorbed to biotite and muscovite. *Environ. Sci. Technol.* **2004**, *38*, 1017−1023.

(9) Nakao, A.; Thiry, Y.; Funakawa, S.; Kosaki, T. Characterization of the frayed edge site of micaceous minerals in soil clays influenced by different pedogenetic conditions in Japan and northern Thailand. *Soil Sci. Plant Nutr.* **2008**, *54*, 479−489.

(10) Kogure, T.; Morimoto, K.; Tamura, K.; Sato, H.; Yamagishi, A. XRD and HRTEM evidence for fixation of cesium ions in vermiculite clay. *Chem. Lett.* **2012**, *41*, 380−382.

(11) Okumura, T.; Tamura, K.; Fujii, E.; Yamada, H.; Kogure, T. Direct observation of cesium at the interlayer region in phlogopite mica. *Microscopy* **2014**, *63*, 65−72.

(12) Betti, M.; Tamborini, G.; Koch, L. Use of secondary ion mass spectrometry in nuclear forensic analysis for the characterization of plutonium and highly enriched uranium particles. *Anal. Chem.* **1999**, *71*, 2616−2622.

(13) McKinley, J. P.; Zeissler, C. J.; Zachara, J. M.; Serne, R. J.; Lindstrom, R. M.; Schaef, H. T.; Orr, R. D. Distribution and retention of Cs-137 in sediments at the Hanford Site, Washington. *Environ. Sci. Technol.* **2001**, *35*, 3433−3441.

(14) Edwards, A. P.; Bremner, J. M. Microaggregates in Soils. *J. Soil Sci.* **1967**, *18*, 64−73.

(15) Tisdall, J. M.; Oades, J. M. Organic-matter and water-stable aggregates in soils. *J. Soil Sci.* **1982**, *33*, 141−163.

(16) Oades, J. M.; Waters, A. G. Aggregate hierarchy in soils. *Aust. J. Soil Res.* **1991**, *29*, 815−828.

(17) Endo, N.; Kimiya, K. Distribution of weathering crust of granitic rocks and alteration of biotite in the middle of Abukuma mountains, northeastern Japan. *J. Jpn. Soc. Eng. Geol.* **1987**, *28*, 1−14.

(18) Kamei, A.; Takagi, T.; Kubo, K. Geology and petrography of the Abukuma granites in the Hiyama district, Fukushima Prefecture, NE Japan. *Bull. Geol. Surv. Jpn.* **2003**, *54*, 395−409.

(19) Maes, E.; Vielvoye, L.; Stone, W.; Delvaux, B. Fixation of radiocaesium traces in a weathering sequence mica → vermiculite → hydroxy interlayered vermiculite. *Eur. J. Soil Sci.* **1999**, *50*, 107−115.

(20) Komarneni, S.; Roy, R. A cesium selective ion sieve made by topotactic leaching of phlogopite mica. *Science* **1988**, *239*, 1286−1288.

(21) National Institute for Materials Science, Database of Promising Adsorbents for Decontamination of Radioactive Substances after Fukushima Daiichi Nuclear Power Plants Accident; http://reads.nims.go.jp/index_en.html.